

Physiological Responses of Frog Vestibular Fibers to Horizontal Angular Rotation

W. PRECHT, R. LLINÁS and M. CLARKE

Dept. of Neurobiology, Max-Planck-Institut für Hirnforschung, Frankfurt (West Germany),
Division of Neurobiology, Dept. of Physiology and Biophysics,
University of Iowa, Iowa City (USA)

Received March 25, 1971

Summary. 1. Single neuronal discharges in frog's vestibular nerve were recorded in unanesthetized preparations with glass microelectrodes. The nerve fibers supplying the horizontal semicircular canal are divided into two types according to the characteristics of their frequency responses to natural stimulation of the horizontal canal. The *afferent* fibers increase their firing rate only on ipsilateral rotation and cease to fire on contralateral acceleration. The *efferent* fibers usually increase their frequencies on rotation in either direction or show an increase in firing on contralateral rotation only. The thresholds of efferent fibers are generally higher as compared to afferent fibers. In addition, most of them show multisensory convergence.

2. Of the afferent fibers 65% showed frequency adaptation in response to prolonged acceleration steps whereas 35% did not show any sign of frequency decrease on prolonged stimulation.

3. Thirty out of 49 afferent units showed a non-linear relation between frequency increase and angular acceleration; in 19 units an approximately linear relationship was noted. In both types of responses the thresholds for frequency increase were in the range between 0.3 — $2.5^\circ/\text{sec}^2$.

4. The time constants of the majority of fibers measured in the linear range were about 3 sec with a range between 1 and 10 sec. It is suggested that fibers having short time constants to acceleration and velocity step input represent acceleration-sensitive units whereas those having long time constants monitor angular velocity. Apparent 'time constants' were adopted for the non-linear range of non-linear units. These values decreased as the acceleration rate increased.

5. An approach to vestibular modeling, based on the present experimental results, is described in the Appendix.

Key Words: Vestibular afferents — Vestibular efferents — Response to rotation — Frog vestibular modeling

Introduction

Single unit activity in the vestibular nerve in response to horizontal angular acceleration was first demonstrated by Lowenstein and Sand (1940a, b) in the isolated labyrinth of elasmobranch. These authors observed that the discharge

frequency recorded in the vestibular nerve fibers from the horizontal canal was related to horizontal rotation, and that the frequency increased during ipsilateral angular acceleration and decreased during opposite rotation, provided that the unit showed a resting discharge. These findings were later confirmed in recordings from the VIIIth nerve of various other vertebrates (Ledoux, 1949; Gernandt, 1949). Further, these electrophysiological data were consistent with the conclusions obtained by direct stimulation of the semicircular canals (Ewald, 1892; Szentágothai, 1950) and were found in general to be in agreement with the torsion pendulum theory of the cupula-endolymph system (Steinhausen, 1931, 1933; Van Egmond *et al.*, 1949; Groen *et al.*, 1952).

During the course of our studies on the responses of cerebellar Purkinje cells of the frog to rotatory stimulation, it became apparent that a detailed study of the characteristics of single elements of the VIIIth nerve of the frog would be an essential prerequisite for the understanding of the Purkinje cell activity reported in the subsequent paper (Llinás, Precht and Clarke, 1971). Previous recordings from the vestibular nerve of the frog were obtained with macroelectrodes which recorded the activity of many units simultaneously (Ledoux, 1949, 1958). This type of recording, however, does not give sufficient information regarding the characteristics of single fiber responses and, as will be discussed in the Appendix, a new form of classification of the functional properties of these fibers is now required. This more detailed division of afferent fibers into acceleration and velocity sensitive prohibits the direct application of the torsion pendulum model proposed by several investigators. On the other hand, the classification of vestibular fibers into level and rate sensitive and the postulation that such changes must be generated by the electrophysiological properties (adaptation) of the peripheral afferent terminal, is very much in keeping with other transducer-encoder systems such as the crustacean stretch receptors (Nakajima and Onodera, 1969a, b).

The present experiments deal with the quantitative aspects of the responses of single afferent and efferent fibers in the VIIIth nerve induced by horizontal rotation. The responses were obtained by applying a constant angular acceleration for a protracted period of time (acceleration step) or sudden arrest after different rates of long lasting constant velocity of rotation (velocity step).

Material and Methods

Experiments were carried out in bullfrogs (*Rana catesbeiana*) weighing 350–400 g following immobilization by intravenous or intralymphatic injection of d-tubocurarine (0.5 mg/kg). The soft tissue covering the skull was infiltrated with procaine before a limited craniotomy was performed in order to expose the intracranial section of the stato-acoustic nerve (VIIIth nerve) (Fig. 1). The skin was kept moist throughout the experiment by covering the animals with a thin layer of wet gauze.

Animals prepared in this manner were then mounted on a Toennies turntable. The head, fixed to a headholder, was placed at the center of the table so as to avoid stimulation of the otolith organs by centrifugal forces. The plane of the headholder was placed such that the horizontal semicircular canals were approximately in the plane of rotation. With the turntable used in the present study, constant horizontal angular accelerations ranging from 0.1–20°/sec² could be applied for a protracted period of time in both directions. The constant velocity could be adjusted to any level between 0 and 200°/sec. Once a desired velocity was obtained, the acceleration was automatically discontinued, and the table rotate at constant velocity. In order to bring the turntable back to zero velocity, two methods were available.

First, the table could be arrested abruptly by activating a brake mechanism, or second, constant rates of deceleration could be selected which would lead to a linear decrease of the angular velocity to zero. Details of the turntable mechanism have been described elsewhere (Shimazu and Precht, 1965). In addition to the horizontal rotation, the apparatus allowed controlled tilting of the mounting frame about the longitudinal and transverse axes. In this study, primarily horizontal rotational stimuli were applied. First, acceleration steps of various magnitudes were given whereby the constant velocity was selected in such a way that the total duration of the acceleration was the same with each test (i. e. with an acceleration of $2^\circ/\text{sec}^2$ the final angular velocity was adjusted to $40^\circ/\text{sec}$, and with $4^\circ/\text{sec}$ it was $80^\circ/\text{sec}$). The constant velocity was then maintained for longer periods of time so that the time course of the decay of discharge frequency to its resting level could be observed. Second, velocity steps or impulses of various magnitudes were applied in most units in addition to the acceleration steps. A given constant velocity was obtained by applying small values of angular accelerations. After the constant level of velocity had been obtained, it was continued for at least 2 min in order to allow the horizontal canal system to return to a steady state, whereupon the brake brought the table to a sudden stop. The brake mechanism was adjusted such that the time it took to reach zero velocity was kept approximately constant (0.5–1.0 sec) with varying stimulus intensities.

Extracellular action potentials from the VIIIth nerve were recorded by means of glass micropipettes filled with 2 or 4 M NaCl with resistances of 5–10 M Ω . They were inserted into the VIIIth nerve in a dorsoventral direction with a micromanipulator. In order to avoid dimpling of the surface of the VIIIth nerve by the microelectrode, the connective tissue covering the nerve was carefully removed from the dorsal surface. The recording preamplifiers were placed on, and moved with, the turntable, and the power supply and output of preamplifiers were connected to the main frame by a circular sliding contact placed along the central axis of the turntable. Action potentials from the VIIIth nerve were led into a two-beam cathode ray oscilloscope through an input cathode follower and a capacity-coupled amplifier (Toennies). The oscilloscope traces were recorded on film with a kymograph camera (Grass) and on FM tape.

Results

Identification and Classification of Vestibular Fibers

In the frog the intracranial section of the VIIIth nerve can be exposed over its entire length without removing the cerebellum. At the point where it leaves the cranium, the main stem of the VIIIth nerve is divided into the anterior and posterior branches which leave the cranial cavity through separate foramina (Fig. 1). The anterior branch contains the fibers supplying the horizontal semicircular canal, as well as the anterior semicircular canal and the otolith organs (Burllet, 1929). The microelectrode recordings to be described here were obtained for the most part from the anterior branch or its proximal continuation, where many fibers were found to respond to horizontal angular acceleration. As a routine procedure, microelectrodes were first inserted into the proximal parts of the nerve region described above and, as the experiment went on, more distal points were selected for insertion. In this way blockage of transmission along the nerve by means of mechanical injury was avoided.

Once a unitary action potential was isolated by carefully advancing the microelectrode into the nerve, horizontal angular accelerations were applied in either direction, and the response of the fiber was first studied qualitatively. Fibers not responding to horizontal rotation were immediately discarded from this study as they were most probably connected to end-organs other than the horizontal canal. The overwhelming majority of the units which showed a distinct response to rotation increased their discharge frequencies during angular acceleration to the side of the recording electrode (ipsilateral rotation). Contralateral rotation pro-

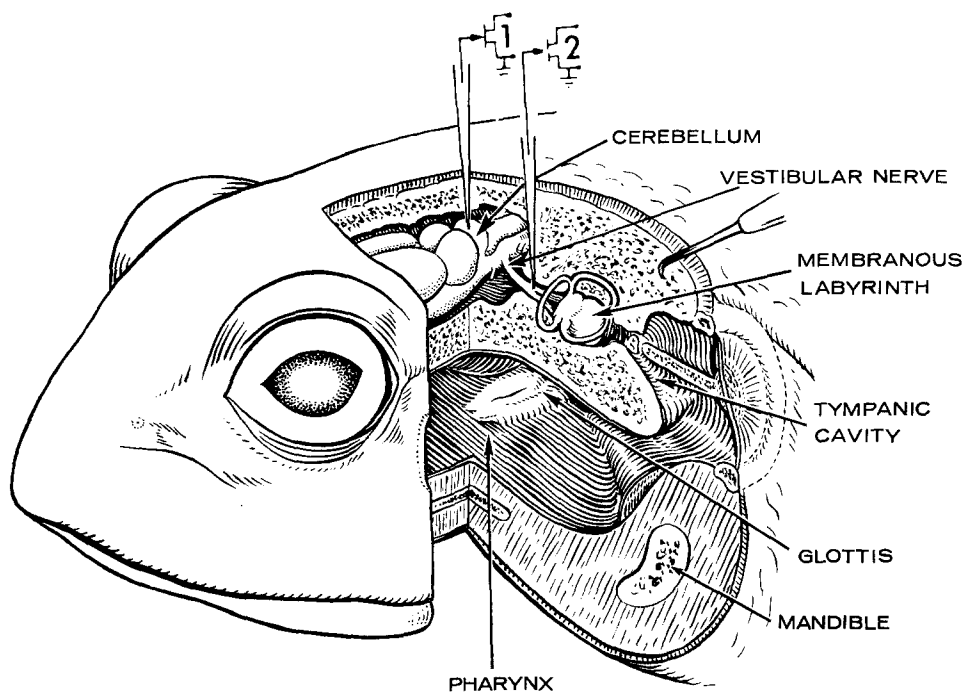


Fig. 1. *Diagram of frog head and brain showing recording sites.* Recording electrodes 1 and 2 are placed in the cerebellum and the VIIIth nerve respectively. Only the intracranial section of the VIIIth nerve was exposed; the peripheral part of the VIIIth nerve and the membranous labyrinth are shown for identification purposes

duced a cessation of the resting discharge, provided that such background firing was present in the unit under study. The results to be reported here are based on 68 single fiber recordings showing this kind of response pattern. Examples of such nerve fibers are given in Figs. 2 and 3. In Fig. 2A a nerve fiber having no resting discharge in the absence of rotation is seen to increase its discharge frequency by ipsilateral acceleration, with a latency of about 2.1 sec. A constant angular acceleration was continuously applied through B and C of Fig. 2. Note that the firing frequency increased continuously until it reached a maximum near the end of trace 2C. Figure 2D depicts a few seconds of recording during constant velocity of rotation, i.e. after the acceleration had been switched off. Accordingly, the firing frequency of the fiber gradually returned to its resting level which in this case was zero. No discharge was observed on contralateral acceleration (not shown in Fig. 2). In Fig. 2E—H the responses of the same fiber to velocity steps are shown. The tests were applied from different levels of contralateral angular velocity (Fig. 2E—H) after the cupula had returned to a position of equilibrium (see Methods). The table was then suddenly arrested at the points indicated by arrows. In each of the recordings shown in Fig. 2E—H, a marked increase in discharge frequencies was observed after the stop. The converse, i. e. no change in discharge frequency, was seen on reversing the direction of the rotatory stimulation. This is exemplified by the results in Fig. 3. In A and B the turntable was brought to a

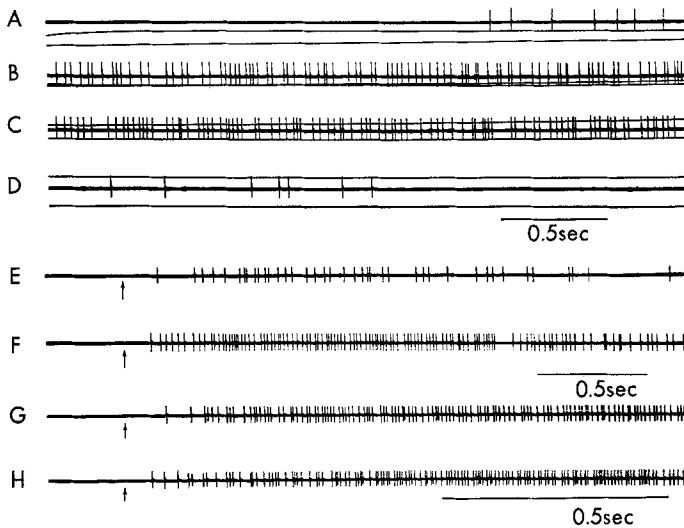


Fig. 2. *Extracellularly recorded discharge of afferent nerve fiber in response to rotational stimulation.* A to D show response of a single fiber to ipsilateral horizontal angular acceleration ($7^\circ/\text{sec}^2$) and constant velocity ($140^\circ/\text{sec}$) of rotation. In A the onset of acceleration coincides with the beginning of the trace showing the action potentials. Acceleration and velocity are monitored by the traces below the recording of the action potentials. B and C were taken 7 and 15 sec respectively after onset of acceleration. Note that the beam monitoring angular velocity has moved above the recording trace. D was taken 6 sec after velocity reached a constant value ($140^\circ/\text{sec}$). E to H show responses of same fiber to sudden arrest after the table had been rotating for 2 min at constant velocities in the contralateral direction ($25^\circ/\text{sec}$ in E, $50^\circ/\text{sec}$ in F, $100^\circ/\text{sec}$ in G and $150^\circ/\text{sec}$ in H). Note difference in time calibration in G and H as compared to E and F

sudden arrest following ipsilateral and contralateral rotation at constant velocities. A point to be stressed is the fact that the duration of the depression of the resting discharge on stopping after ipsilateral rotation was approximately equal to the duration of the increase of firing rate which followed stimulation in the opposite direction.

Since the horizontal semicircular canal was the only end-organ stimulated in these experiments (see Methods), and since the response pattern of the fibers described above is in perfect agreement with the direction specificity of the cupula and the pattern found in fibers from the horizontal canals of other vertebrates (Lowenstein and Sand, 1940a, b; Ledoux, 1949; Trincker, 1965), it is safe to assume that they represent the first order neurons of the horizontal canal. The possibility exists, however, that some of the responses reported above are derived from efferent vestibular fibers. In a previous paper by Llinás and Precht (1969), it has been shown that a small number of efferent fibers recorded in the nerve could be activated trans-synaptically with short latencies by stimulating the VIIIth nerve electrically, suggesting a feedback loop from an end-organ through the central nervous system onto itself. On natural stimulation, however, these efferent fibers have generally higher thresholds as compared to afferent fibers (Schmidt, 1963; Llinás and Precht, 1969). Further, as will be reported in the last section of this paper, many of the efferent fibers can be activated by rotation in either

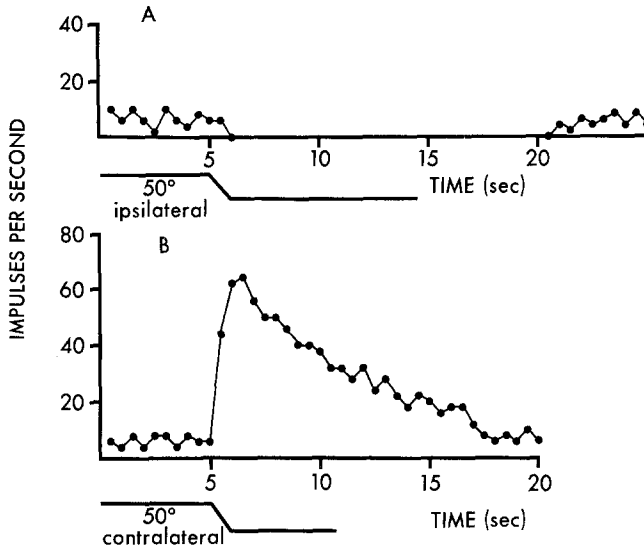


Fig. 3. Frequency diagrams of discharges of single afferent fiber in response to sudden arrest of rotating turntable. In A and B, constant velocities of horizontal rotation ($50^\circ/\text{sec}$) were applied for 2 min in the ipsilateral and contralateral direction, respectively. At the time indicated by downward deflection of the velocity line (below each frequency diagram), the table was brought to a sudden arrest. Ordinates give impulses per second

direction and are found to be highly susceptible to stimulation other than labyrinthine. In conclusion it may be said that the overwhelming majority of the fibers that increase their firing rate on ipsilateral angular acceleration, and decrease on contralateral rotation with thresholds that are lower than $2^\circ/\text{sec}^2$, are indeed primary vestibular fibers signalling horizontal canal activity. Action potentials from fibers that respond with an increase in discharge frequency on acceleration in either direction, and which show multi-sensory convergence, are incompatible with the cupula mechanics worked out by Lowenstein and Sand (1940a, b) in the *isolated* labyrinth and are thus considered efferent fibers. The responses of the afferent nerve fibers will be described first.

Responses of Afferent Fibers to Horizontal Angular Acceleration of Long Duration

Most of the single unit recordings in the present experiments were stable for long time periods so that application of constant angular acceleration of long duration was possible. Since angular accelerations are regarded as an adequate stimulus for semicircular canal receptors, a protracted period of constant acceleration such as used in the present study should be applied in order to determine whether there is any adaptation (i. e. frequency decrease of vestibular impulses during long lasting constant stimulation). Slight adaptation has been observed in fibers of the VIIIth nerve of *Raja clavata* by Lowenstein (1955) using exponentially increasing D.C. currents, thus simulating the slow exponential change of cupula deflection caused by angular accelerations. In recording mass activity from the VIIIth nerve of the frog with macroelectrodes, Ledoux (1949, 1961) observed a decrease in activity on prolonged application of constant angular acceleration.

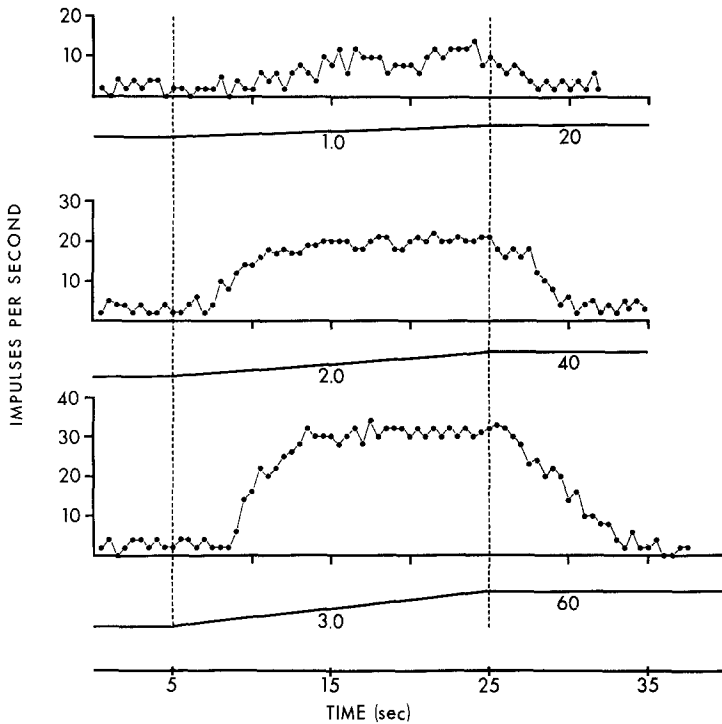


Fig. 4. Frequency diagrams of discharges of an afferent fiber in response to ipsilateral constant angular accelerations. In each diagram the ordinate represents spikes per second of single unit discharges measured in each half-second. Onset of acceleration is indicated by left vertical broken line, and cessation of acceleration (or beginning of constant velocity rotation) by the right vertical broken line. The line below each frequency diagram indicates velocity of rotation. The left-hand number in each diagram indicates the acceleration rate, and the right-hand number the velocity of constant rotation

In the present experiments, however, it was found that approximately 35% of the fibers from the horizontal canal did not show any significant adaptation in response to constant angular accelerations of long duration. This is exemplified by the primary fiber response illustrated in Fig. 4. The duration of the angular accelerations in Fig. 4 was 20 sec in each of the frequency diagrams. In each of the diagrams the frequency of discharge increased along an approximate exponential time course and reached certain maximal values whose levels were dependent on the rate of acceleration applied. The maximum level of discharge was maintained constant during the remainder of the acceleration. On termination of the angular acceleration, or after the onset of constant velocity of rotation, the discharge frequencies returned to control levels. The value of 20 sec for the duration of the stimulus is by no means the limit beyond which adaptation may occur. In several units, lack of adaptation has been observed even after stimuli of three times that duration. Parenthetically it should be mentioned that constant angular accelerations of such duration are, of course, unphysiological and would never occur under biological conditions. The presence of non-adapting vestibular nerve fibers should be emphasized, particularly since Ledoux's data would tend to suggest the opposite.

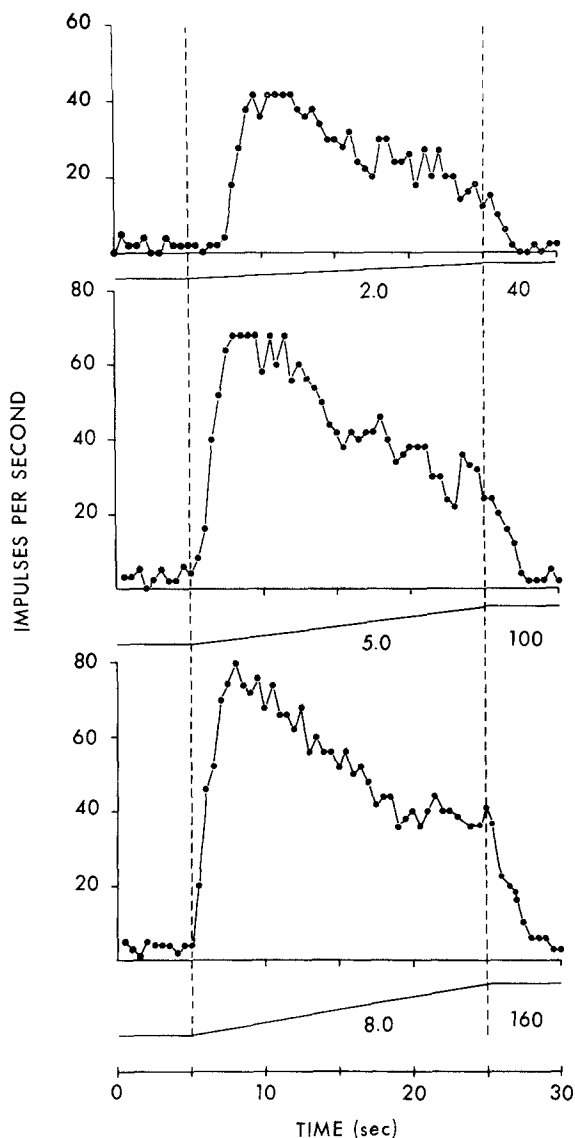


Fig. 5. Frequency diagrams of discharges of an adapting afferent fiber in response to ipsilateral constant angular accelerations. Arrangement of diagrammatic representation is the same as in Fig. 4

As mentioned above, approximately 65% of the fibers studied showed frequency adaptation during constant angular acceleration. This kind of response pattern is illustrated in Fig. 5. In each of the frequency diagrams of this figure, a frequency decline was noted in response to different rates of constant accelerations applied for periods of 20 sec. The magnitude of the response decline varied from unit to unit, ranging from barely visible adaptation to complete return to the level of resting discharge.

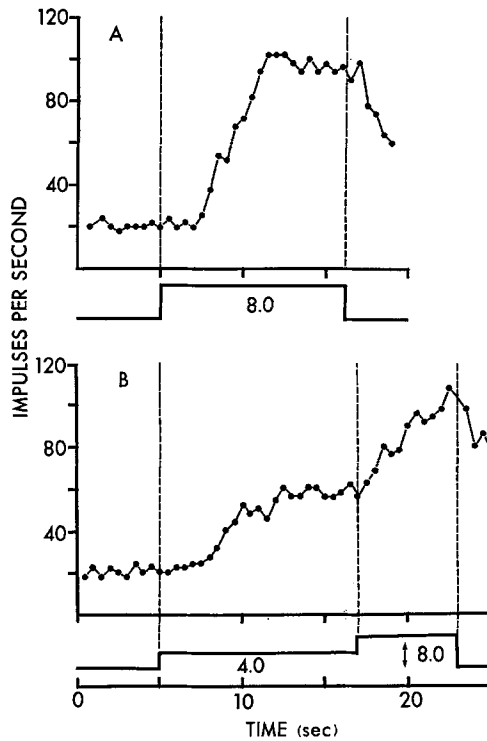


Fig. 6. Response of non-adapting fiber to single and double steps of acceleration. A, frequency diagram of fiber in response to ipsilateral constant horizontal angular acceleration ($8^{\circ}/\text{sec}^2$). Left and right hand vertical broken lines and curve below diagram indicate beginning and cessation of acceleration, respectively. B, frequency diagram of same fiber in response to two successive steps of acceleration (4.0 and $8.0^{\circ}/\text{sec}^2$). Broken lines mark beginning and end of different acceleration rates

In non-adapting units, superimposed sequential stimulation by means of acceleration steps demonstrated a linear addition of the responses. As illustrated in Fig. 6A, a single acceleration step ($8^{\circ}/\text{sec}^2$) was applied for approximately 12 sec, and resulted in a response with a frequency of 80 impulses/sec. In B of the same figure an acceleration step of $4^{\circ}/\text{sec}^2$ was applied first and was followed by a second step of the same magnitude totalling an acceleration of $8^{\circ}/\text{sec}^2$. Comparing records A and B it becomes apparent that the final frequency obtained by adding two steps of $4^{\circ}/\text{sec}^2$ was very close in magnitude to that obtained by a single stimulus of $8^{\circ}/\text{sec}^2$. Very much in contrast with this situation was the lack of summation of superimposed stimuli in adapting units (Fig. 7). In this case the second stimulus barely changed the firing frequency of the unit. It is important to emphasize that the linearity of the response, which relates to the monotonic relationship between the amplitude of the stimulus and the magnitude of the response, does not seem to be correlated with the presence or absence of adaptation.

Relation Between Frequency Increase and Intensity of Stimulation

The frequency response of afferent fibers during horizontal angular accelerations of increasing intensity showed a clear relationship not only to the accelera-

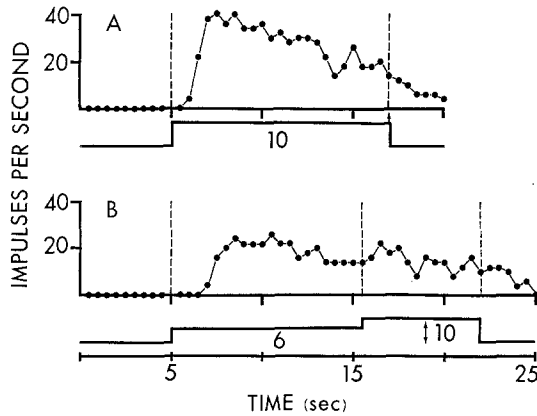


Fig. 7. Response of an adapting vestibular fiber to single and double steps of accelerations. Arrangement of diagrammatic representation is the same as in Fig. 6

tion as such but also to the magnitude of stimulation (Figs. 4, 5, 11). Forty-nine fibers were individually tested with approximately 6 different rates of acceleration (ranging from 0.2 — $10^\circ/\text{sec}^2$) and their response curves plotted as illustrated in Figs. 4, 5 and 11. In all cases sufficient time (about 3 min) was permitted to elapse between tests in order to allow for a complete recovery from the preceding stimulation. This procedure was found necessary since rapid successions of several tests, each lasting some 40 sec, caused "fatigue" of the response as judged from the gradually decreasing firing rates. With this variable in mind, the average resting discharge was determined before the onset of each stimulation and was subtracted from the average of the peak frequency value produced by a given constant angular acceleration. This subtracted value was plotted against the acceleration. Of 49 afferent fibers analyzed in that manner, 30 units showed a non-linear relation between frequency increase and acceleration in the range between 0.2 and $10^\circ/\text{sec}^2$. Examples of such fibers are illustrated in the right hand diagram of Fig. 8 where the above defined frequency increases are plotted against the logarithmic scale of acceleration.

The gradients of the regression lines of the activity in the afferent fibers varied over a relatively wide range, indicating that the responsiveness of afferent fibers to accelerations of the same values shows considerable differences. No relation existed between the level of resting discharge and the gradient of the regression lines as it was described for second order vestibular neurons of the cat (Shimazu and Precht, 1965). In 19 units, on the other hand, an approximately linear relationship has been observed between frequency increase and rate of acceleration. Examples of such fibers are illustrated in the left-hand diagram of Fig. 8 where the frequency increase was plotted against the linear scale of acceleration. In some units the individual values showed too much variation and were thus discarded from the quantitative treatment of the present material.

The points where the regression lines cross the abscissae in Fig. 8 indicate the threshold for the frequency increase in each afferent fiber. In the case of units which showed spontaneous discharge in the absence of any rotatory stimulus, precise determination of the threshold is difficult because a slight fluctuation of the resting

discharge interferes with the identification of the small response. Lowenstein (1956) has suggested that theoretically a threshold hardly exists at all in spontaneously firing units, which would mean that the regression lines of Fig. 8 might not be straight in the region close to the X-axis and may rather extend to zero. In the face of this argument, the frequency diagrams obtained with subthreshold values, as defined above, were analyzed with special care. In most of the units no statistically significant changes in impulse frequency were observed. Thus, it may be said that the determination of threshold, as described above, gives satisfactory values

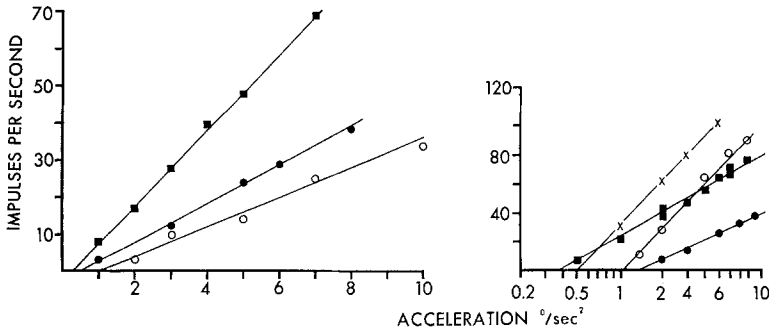


Fig. 8. Relation between angular acceleration and maximum frequency increase of afferent fibers. In each of the diagrams, regression lines connect the points obtained from a single fiber by subtracting the resting discharge from the average of the maximum frequency increase. Note semilogarithmic plot of right hand diagram

for both tonically active and silent fibers. The threshold values for different afferent fibers ranged from 0.3 – $2.5^\circ/\text{sec}^2$ with a peak between 0.5 and $1.5^\circ/\text{sec}^2$. These values are well within the range found in central vestibular neurons in cats (Shimazu and Precht, 1965), indicating that in widely separated vertebrates the horizontal canal system has a very similar sensitivity in response to angular acceleration. Furthermore, the gradients of the regression lines of the input-output diagrams of Fig. 8 are similar to the ones described for second order vestibular neurons of the cat.

Input-output diagrams of single afferent fibers were also obtained by applying velocity steps or impulse-like stimulation (see Methods). Examples of such diagrams are shown for a linear unit in Fig. 10D and a non-linear unit in Fig. 13C. As the magnitude of stimulation increased (generally above $100^\circ/\text{sec}$) the increases in impulse frequencies of linear units began to level off as well, indicating that even in these fibers a non-linear response can be observed at the upper ranges. The highest peak frequency found in this study was 180 impulses/sec; the stimulus was an impulse of $200^\circ/\text{sec}$.

Modulation of the Discharge Frequency in Response to Acceleration and Velocity Steps

At resting condition, many afferent nerve fibers showed spontaneous firing that varied between 2 and 35 impulses/sec. The majority of these spontaneous units, however, were characterized by a low level resting discharge (below 15/sec); others demonstrated no detectable resting discharge. Examples of this latter type

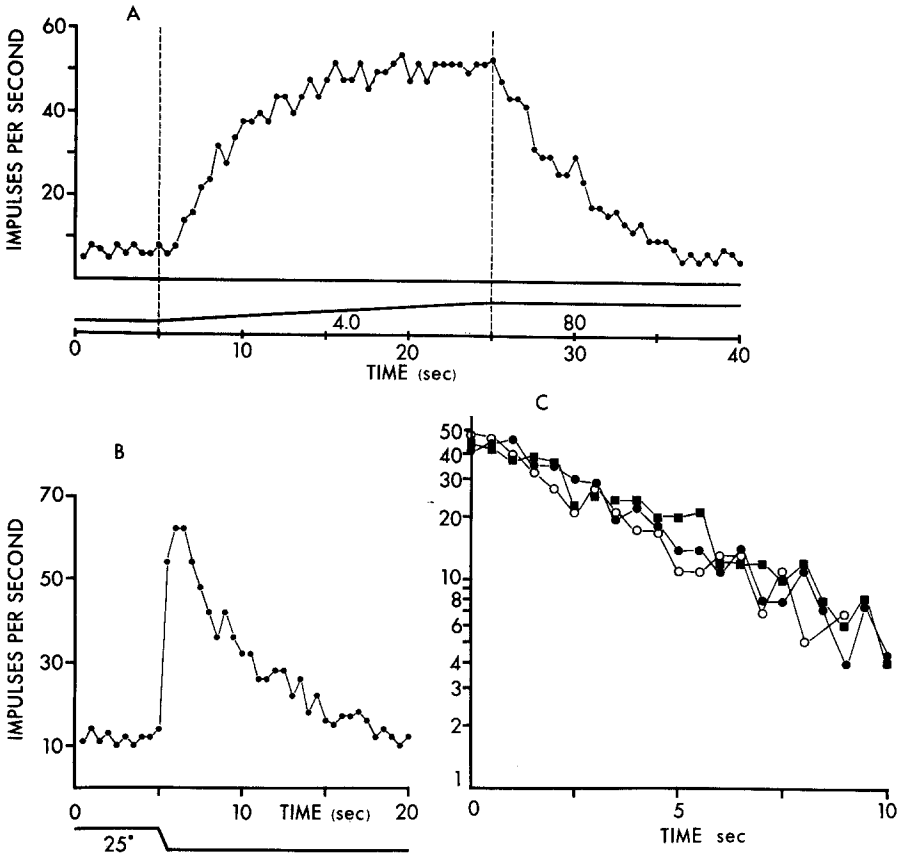


Fig. 9. Responses of linear afferent fiber to acceleration and velocity steps. A, frequency diagram of discharge of afferent fiber in response to constant horizontal angular acceleration, as illustrated in Fig. 4. B, response of same fiber to sudden arrest of table after constant velocity (25°/sec) of rotation in the contralateral direction. Downward deflection of curve below the diagram indicates onset of cessation of rotation. C, semilogarithmic plot of impulse frequency during rising phase (filled circles) and falling phase (squares) of acceleration step shown in A and the falling phase of velocity step (open circles) shown in B. Abscissa: time in seconds. Ordinate: impulses per second

of fiber can be seen in Figs. 1, 7 and 11. Since it is obviously much more difficult to detect silent units, a comparison between the number of tonic and silent fibers does not appear to be a very reliable index of the true population of these two types, and it may well be that both patterns are equally distributed in the nerve of the horizontal canal. It should be noted also that the level of resting discharge of a single fiber could change during a long recording period, as can be seen in Figs. 9 and 14. The reason for such changes might be inherent in the receptor-nerve fiber junction, or else they may be brought about by changes in the activity of the efferent vestibular system which is known to influence afferent fiber discharge (Llinás and Precht, 1969).

Linear units in Figs. 4 and 9A illustrate plots of the afferent fiber impulse frequencies during ipsilateral horizontal angular accelerations of various amplitudes.

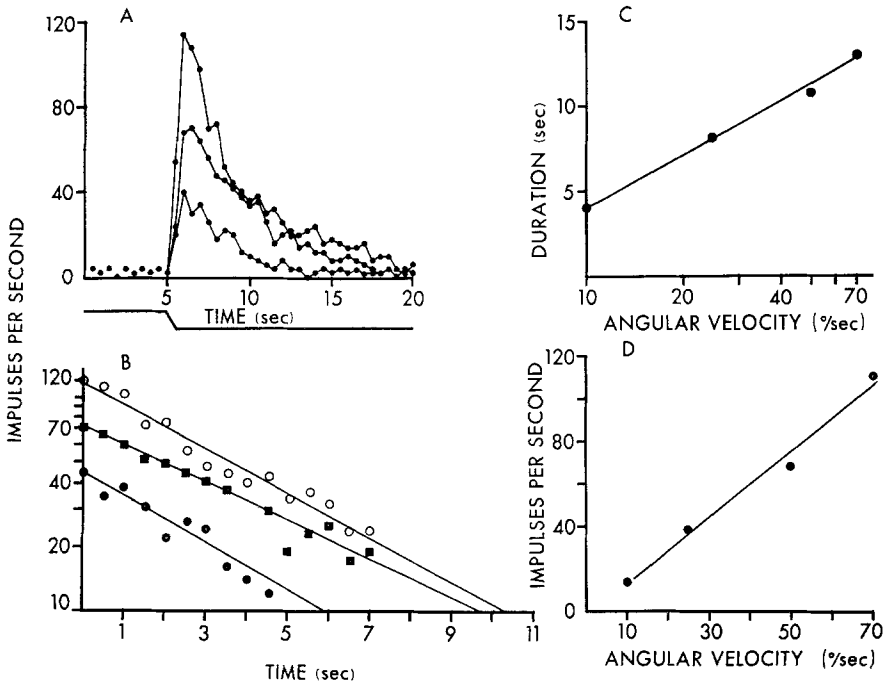


Fig. 10. Frequency diagrams of linear afferent fiber in response to velocity steps and relation between rate of velocity and duration of responses. A, responses of single fiber to velocity steps („impulses“) of varying magnitudes (25°/sec, 50°/sec, 70°/sec). Onset of cessation of rotation is indicated by deflection of curve below the diagram. B, semilogarithmic plot of impulse frequencies of falling phases of the curves shown in A. Filled circles refer to the lower, square symbols to the middle, and open circles to the upper curve shown in A. C, semilogarithmic plot of duration of responses against velocity steps of various magnitudes. D, relation between rate of angular velocity and maximum increase of frequency of single unit discharge

As shown in each of these diagrams, the discharge frequencies increased along an approximately exponential time course to a peak value which was maintained during the remainder of the constant accelerations. Generally, the time interval between onset of rotation and commencement of frequency increase was directly related to amplitudes of accelerations, although exceptions to this rule were seen (e. g. Fig. 4, middle and lower diagrams). Since slight deviations from a linear increase in angular velocity of the turntable are present within the first few seconds of rotation (see Shimazu and Precht, 1965), no systematic treatment of the latencies for frequency increase were made in the present experiments.

As far as responses to constant velocity are concerned, in all cases studied the discharge frequency decayed along an approximately exponential time course once the constant velocity was reached (Figs. 4, 9A). In Fig. 9C the increasing and decreasing phases of the response to the constant acceleration were replotted on a semi-logarithmic scale. In addition, the decay phase of the same unit following a velocity step stimulation (Fig. 9B) was plotted in Fig. 9C. All points were distributed along an approximately straight line with a time constant of 4.5 sec. The frequency diagrams of another linear unit in response to velocity steps of

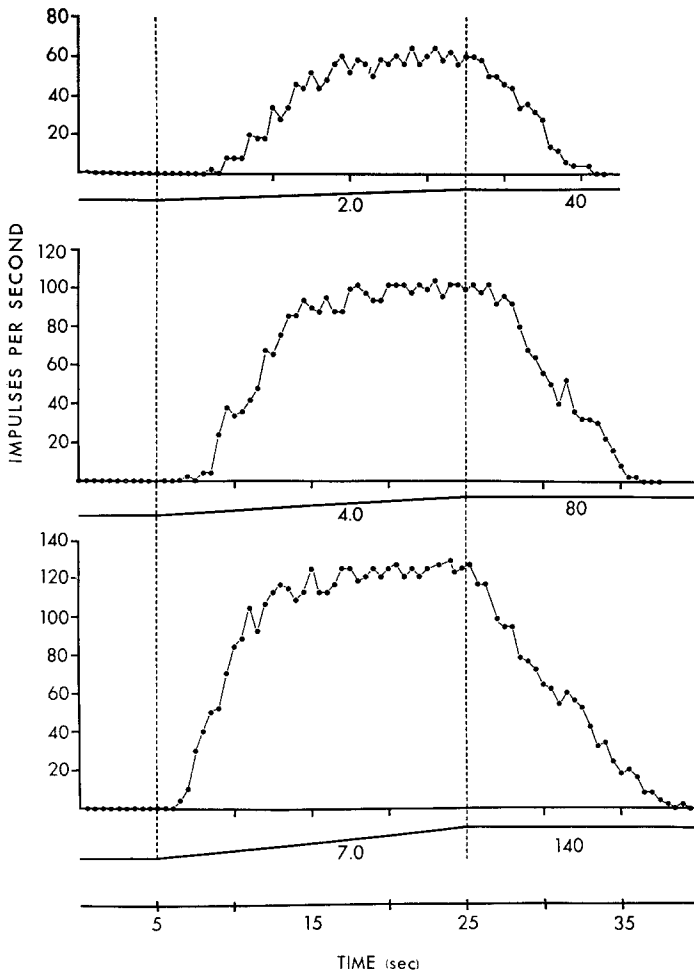


Fig. 11. Frequency diagrams of afferent fiber in response to horizontal angular accelerations showing decrease of "time constant" with increasing acceleration. Arrangement of diagrammatic representation is the same as in Figs. 4, 5 and 9

varying magnitudes are illustrated in Fig. 10 and the linear input/output diagram of the unit is shown in Fig. 10D. In Fig. 10B the falling phases of the three frequency curves of Fig. 10A were replotted on a semi-logarithmic scale. The time constants of the responses to three different velocity steps were found to be similar (3.7, 4.0 and 3.3 sec) from the top to the bottom, respectively. Similarly, the time constants of the increased firing rate during constant accelerations were constant in linear units over the range tested ($0.2-10^2/\text{sec}^2$). This is shown for two units in Fig. 12B by the points connected by the broken lines. As one would expect from previous investigations, the durations of the responses of single fibers to velocity steps of different magnitudes are proportional to the logarithm of the angular velocity as shown in Figs. 10C and 13B (Ledoux, 1958).

In Fig. 11 are shown the frequency diagrams of an afferent fiber that is characterized by a non-linear acceleration frequency relationship. Some features of this

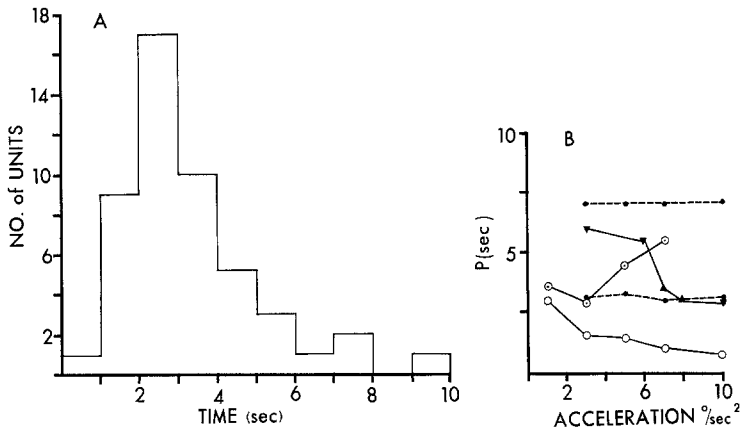


Fig. 12. *Time constants of frequency responses of afferent fibers to ipsilateral horizontal angular acceleration.* A, histogram of time constants of responses of fibers to constant horizontal angular acceleration measured in the linear range of the units. B, relation between acceleration rate and time constants for different fibers. Broken lines connect points obtained from two linear units. Open circles and triangles represent measurement of time constants of rising phase obtained from two non-linear units. Note decrease of "time constant" as acceleration rate increases. Dotted circles show the time constant of the falling phase of same unit whose time constant of the rising phase is illustrated by open circles

unit, such as the low threshold for frequency increase and the non-adaptive behavior, are similar to the linear units shown in Figs. 4 and 9C. There is, however, a marked difference in the time course of the rising phases of the frequency increases to constant angular accelerations as demonstrated in Fig. 11. To allow a comparison between the properly determined time constants of the linear units, in non-linear units the time that was necessary to reach 63% of the average peak frequencies was measured in the linear range of the non-linear units and the values thus obtained were adopted as a rough approximation of the time constant. These values and the time constants of the linear units are combined in the histograms of the frequency distribution of the time constants of afferents fiber in response to horizontal angular acceleration (Fig. 12A). The majority of the fibers have time constants of about 3 sec. Further consideration will be given to this finding in the Discussion and in the Appendix.

In order to compare with the linear units the time courses of non-linear units in non-linear ranges, an apparent "time constant" (p) was arbitrarily defined. For the rising phase of a response, p was defined to be the time necessary to reach 63% of the average peak frequency, and for the falling phase the time to reach 37% of the average peak frequency.

In Fig. 12B, time constants of linear units and the apparent "time constants" of non-linear units are plotted against the acceleration. As expected, the time constants of the linear units did not change with different rates of acceleration (broken lines), whereas the apparent "time constants" of the non-linear units showed considerably smaller values with increasing stimulation (open circles and triangles). The dotted circles show that the "time constant" of the falling phase of the response to constant angular acceleration of a non-linear unit increases with an increase in

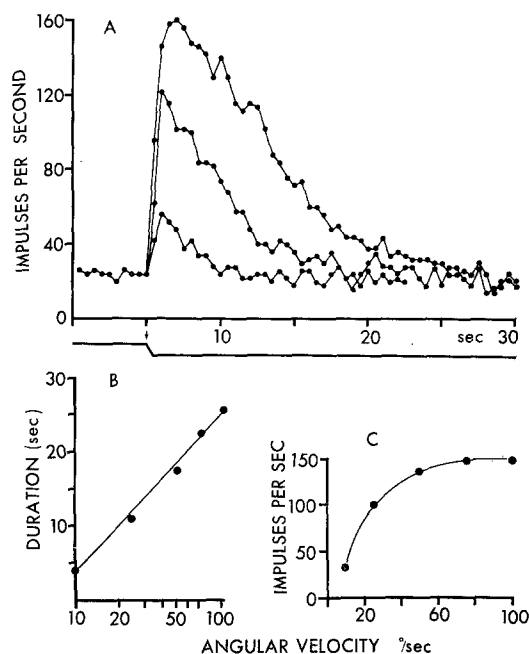


Fig. 13. Frequency diagrams of discharges of non-linear afferent fiber in response to velocity steps; relation between rate of velocity and duration of response. A, responses of fiber to velocity steps of varying magnitudes ($10^{\circ}/\text{sec}$, $25^{\circ}/\text{sec}$, $50^{\circ}/\text{sec}$). Table was rotating at constant velocity in the direction contralateral to the recording electrode. B, semilogarithmic plot relating duration of response and rate of angular velocity before cessation of rotation. C, relation between rate of angular velocity and maximum frequency of single fiber discharge

acceleration rate. In Fig. 13 frequency diagrams are given for a non-linear unit in response to velocity steps. The non-linearity of the input-output relationship is shown in Fig. 13C where the peak impulse frequencies in response to different velocity steps are plotted against the angular velocity. Three samples illustrating the whole time course of the responses are shown in Fig. 13A.

On the So-called Undershoot

It is well known that velocity steps of higher magnitude cause not only the usual post-rotatory nystagmus that is to be expected on the basis of the cupula mechanisms but also, on occasion, a secondary phase of after-nystagmus whose direction is opposite to the usual post-rotatory nystagmus can be observed (Jung and Kornhuber, 1964). These phases of after-nystagmus are paralleled by frequency oscillations observed in single second-order vestibular neurons of the cat (Shimazu and Precht, 1965). The fact that both in fish (Groen *et al.*, 1952) and in frogs (Ledoux, 1958) the discharge frequencies of some of the primary vestibular fibers show an undershoot in response to strong velocity steps, makes it difficult to ascribe the phenomenon entirely to central mechanisms. Theoretically, there might be the possibility that the undershoot is caused by the action of efferent vestibular fibers on the sensory hair cells in the cristae. This explanation, however, does not hold in the case of the experiments performed in fish that have been done on isolated

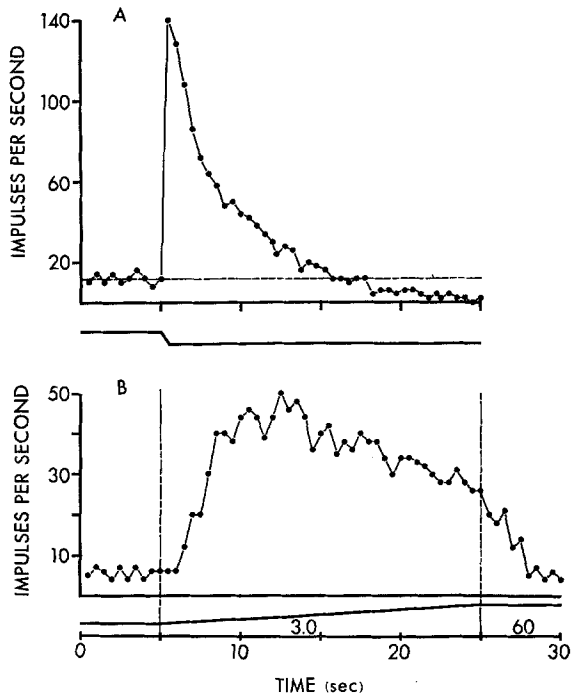


Fig. 14. Frequency diagrams of afferent fiber in response to velocity and acceleration steps showing "undershoot". A, velocity of rotation before sudden arrest was $150^\circ/\text{sec}$. Cessation of rotation is indicated by downward deflection of curve below the diagram. B, response of same unit to constant angular acceleration ($3.0^\circ/\text{sec}^2$). Note adaptation of response. Vertical broken lines indicate onset and cessation of acceleration

labyrinthine preparations. Furthermore, serious problems arise by virtue of the fact that undershoots of the impulse frequency following a velocity step are incompatible with the prevailing theory that the cupula is an overcritically damped torsion pendulum (Steinhausen, 1931, 1933; Groen *et al.*, 1952). We, therefore, have critically examined our material for the existence of single fibers showing the undershoot phenomenon. The overwhelming majority of the fibers did not show any significant undershoot as can be seen in Figs. 3, 10 and 13. In several cases, however, undershoot has been observed in response to strong velocity steps. The unit in Fig. 14A and B is shown to respond to a velocity step of $150^\circ/\text{sec}$ (A) and to an acceleration step (B). Following an increase in frequency of discharge immediately after the arrest of rotation (A), the discharge decays and passes the control level indicated by the broken line, thus showing an undershoot. Closer inspection of the resting level shown in Fig. 14A and B, however, reveals a discrepancy in the firing level which is about 12/sec in A and about 5/sec in B. This slight change in resting level of firing during high speed constant angular rotation has been seen in most of the units that showed an undershoot. The mechanism for the change in the level of resting discharge during high speed constant angular rotation is unclear at the present time, and it is not known if similar changes would occur in isolated laby-

rinthine preparations. Given the fact that this change occurred in the unit illustrated in Fig. 14, undershoot might simply be explained as a return of the firing frequency to its true resting level. In addition to this effect, only a small fraction of the phenomenon might be due to a true undershoot. Interestingly, most of the cells showing this undershoot demonstrated (as seen in Fig. 14) a certain degree of adaptation, which seems also to be the case for second-order vestibular neurons in other species (Shimazu and Precht, 1965).

Finally, in silent fibers an overshoot of discharge following a period of undershoot which, of course, could not be seen in recording spike frequency, has never been observed in our material. In central vestibular neurons, however, such overshoots have been reported for silent neurons (Shimazu and Precht, 1965). From our material in the frog, we cannot reject the occurrence of an undershoot. We would like to emphasize, however, that it occurs only in a few neurons and that even in these cases, the effect was not distinct enough to justify considering it as a functionally important feature of afferent fibers.

Responses of Efferent Vestibular Fibers to Rotation

In recording from the VIIIth nerve of the frog, fibers were occasionally found whose response pattern to horizontal rotation could not be explained on the basis of the cupulaendolymph mechanisms. It is well known from the studies of Lowenstein and Sand (1940 a, b) on the isolated labyrinth of fish that afferent fibers of the horizontal canal increase their discharge frequencies on ipsilateral acceleration, i. e. on utriculopetal deviation of the cupula. The converse, a decrease in firing rate, is found on contralateral angular acceleration which leads to an utriculofugal deviation of the cupula. No exceptions to this rule have been seen in the isolated preparation of the end-organs and the VIIIth nerve. On the basis of these findings, it may be assumed that responses other than the ones found in the isolated preparation are derived from efferent vestibular fibers. In the frog the existence of efferent fibers terminating on the sensory hair cells of the labyrinth has been demonstrated both anatomically (Hillman, 1969) and physiologically (Gleisner and Henriksson, 1963; Schmidt, 1963; Llinás and Precht, 1969).

Functionally these vestibular nerve fibers demonstrate an increase in discharge frequency during rotation in either direction. This is illustrated by the frequency diagrams of two such fibers shown in Fig. 15. In Fig. 15A, B, E and F acceleration steps of the same magnitudes have been applied in the ipsilateral and contralateral direction, resulting in both cases in an increase of firing rate which is correlated with the acceleration and which begins to fall off as soon as the constant velocity is reached. The falling phase of Fig. 15A is considerably irregular and prolonged, a finding which is often observed in efferent nerve fibers. Since these neurons are of central origin and are known to show multi-sensory convergence, extralabyrinthine inputs might be responsible for the delayed fall-off in frequency of discharge. From the point of view of threshold, significantly higher rates of angular acceleration were necessary to activate these fibers as compared to the afferent fibers. An exceptionally low threshold (approximately $1.0^\circ/\text{sec}^2$) was found in one of the units illustrated in Fig. 15E and F. About half of the units recorded showed spontaneous discharge in the absence of rotatory stimulation (Fig. 15E and F.)

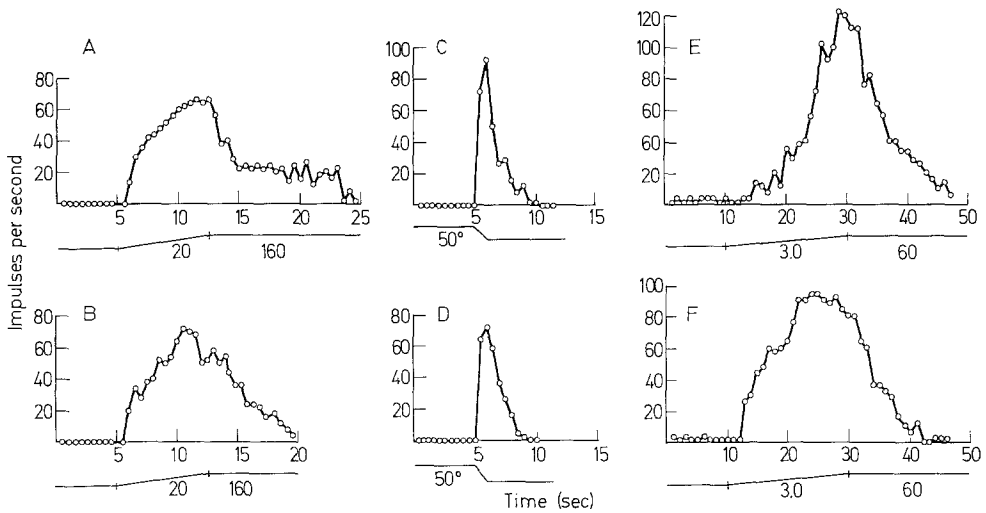


Fig. 15. Frequency diagrams of efferent vestibular fiber in response to angular accelerations. A and B, responses of same fiber to ipsi- and contralateral horizontal angular accelerations ($20^\circ/\text{sec}^2$) respectively. C and D, responses of same fiber to sudden arrest of ipsi- and contralateral rotations at constant velocities ($50^\circ/\text{sec}$). E and F, responses of another unit to ipsi- and contralateral constant horizontal angular accelerations ($3.0^\circ/\text{sec}^2$), respectively. Note spontaneous activity and low threshold

The same fiber shown in Fig. 15 A and B was also tested with velocity steps as illustrated in Fig. 15 C and D. Slight asymmetries are noted in the peak response as well as in the falling phase. Similar asymmetries in the peak responses to ipsi- and contralateral rotation are seen in Fig. 15 E and F. Since the frequency increase caused by contralateral rotation must be generated by impulses arising from the contralateral labyrinth which eventually reach the efferent neuron through multisynaptic chains, such directional asymmetries are not surprising.

On occasion slightly different response patterns, which are presumably ascribable to efferent fibers, were observed. Thus, some units showed only a weak or no response on ipsilateral rotation, whereas contralateral rotation gave a clear-cut frequency increase. It may be suggested that in these cases the efferent neuron was primarily connected to the contralateral side. Central neurons of this type have been described in the vestibular nuclei of the cat by Shimazu and Precht (1965). Finally, as already mentioned above, some of the high threshold afferent fibers that increase their firing rate on ipsilateral rotation and cease to fire on contralateral acceleration may be efferent in nature, although no proof exists at the present time for this hypothesis. The short latency trans-synaptic activation of efferent fibers following electrical stimulation of the VIIIth nerve reported by Llinás and Precht (1969) and recorded intracellularly at the auricular lobe level, would however tend to support the presence of a feed-back loop consisting entirely of structures located on the ipsilateral side of the brain stem.

As already mentioned above, most efferent vestibular fibers showed multi-sensory convergence, i. e. they responded to a varying extent to stimuli other than labyrinthine. Similar findings have been described by Schmidt (1963), Klinke

(1970), and Dichgans *et al.* (1970). Passive movement of the extremities and gentle touch of the skin, particularly around the head, frequently caused changes in frequency of efferent neurons. This finding may suggest that the efferent cells can be influenced through multisynaptic chains of neurons by several sensory systems. Some of the functional implications of these efferent systems will be discussed later.

Discussion

It can be concluded from the above results that the nerve fibers supplying the horizontal semicircular canal of the frog are divided into two types according to the characteristics of their response to natural stimulation of the horizontal semicircular canal. The afferent nerve fibers increase their firing rate only on ipsilateral rotation and cease to fire on contralateral acceleration. The efferent nerve fibers usually increase their firing rate on rotation in either direction or show an increase in firing on contralateral rotation only.

The response characteristics of the afferent neurons will be discussed first. Qualitatively speaking, their responses are in complete agreement with the results obtained by Lowenstein and Sand (1940a, b) in elasmobranch and by Germandt (1949) in the cat vestibular nerve. As in all other vertebrates the afferent vestibular fibers reflect the directional sensitivity of the hair cells in the crista semicircularis horizontalis which are probably depolarized by endolymph cupula movements in the direction of the utricle (utriculopetal) and are hyperpolarized by endolymph movements bending the hairs in the opposite direction (utriculofugal).

The main aim of this study was to determine some of the dynamic characteristics of afferent vestibular nerve fibers. Except for the work done by Lowenstein and Sand (1940a, b) in fish, no quantitative data are available on single unit analysis of the VIIIth nerve of other vertebrates. Such data are, however, important for a better understanding of the peripheral vestibular mechanisms which in the past have been deduced from human psychophysical experimentation and from vestibular induced ocular nystagmus. The present experiments have demonstrated that the individual vestibular afferent fibers show such a variety of response characteristics that mechanical properties of the viscoelastic cupula-endolymph system cannot be derived from them. Since anatomically only one basic type of hair cell is found in the frog (Hillman, 1969), these disparities may be generated by differences in the functional properties at the initial portion of the afferent fiber system. The transmission from hair cell to afferent fibers, which is most likely chemical, should otherwise be similar for all fibers. Such differences between properties of peripheral afferent axons have been reported for other receptor systems (Nakajima and Onodera, 1969a, b).

Attempts to model the dynamic properties of the responses obtained from stimulation of the horizontal canal system should take into consideration the functional characteristics of the single fiber responses. One such approach to vestibular modeling is described in the Appendix to this paper. In addition, the differences between this model and previous ones are critically evaluated. As described in the Appendix, it is proposed that fibers having short time constants to acceleration and velocity step inputs might represent acceleration sensitive units whereas afferent fibers having long time constants monitor velocity. Further-

more, it should be emphasized that the majority of afferent fibers showed a non-linear relation between frequency increase and angular acceleration in the range between 0.2 and $10^\circ/\text{sec}^2$. These results are similar to the data obtained with second order vestibular neurons and abducens motoneurons of the cat using the same range of angular accelerations as in the present experiments.

Generalization of a linear stimulus response relationship in the equilibrium system proposed by Schoen (1957) and implicitly assumed in attempts to model the vestibular system does not appear to us to be acceptable. As for the problem of frequency adaptation of afferent fibers, recordings of mass activity from the nerve of the horizontal canal by Ledoux (1949, 1958, 1961) show the existence of adaptation. The present experiments based on single fibers recordings, however, show that in about 35% of the units no significant frequency adaptation can be found in response to constant angular acceleration of long duration. In central vestibular neurons of the cat an even higher percentage of neurons was found to be non-adaptive under similar experimental conditions (Shimazu and Precht, 1965; Precht *et al.*, 1967, 1969), suggesting that non-adapting neurons play an important role in the peripheral and central parts of the vestibular system in different species. Given that most angular rotations occurring in normal life are of short duration, frequency adaptation probably is of little functional importance in the horizontal canal system.

The lowest thresholds for frequency increase of single afferent fibers in the frog in response to horizontal angular accelerations were approximately $0.3^\circ/\text{sec}^2$. Thus, their thresholds are within the same range as the thresholds determined for second order vestibular neurons and ocular motoneurons in the cat (Shimazu and Precht, 1965; Precht *et al.*, 1967, 1969) and for human sensation of rotation and per-rotatory ocular nystagmus (for summary see Clark, 1967; Jung and Kornhuber, 1964). These findings stress the functional similarities of the vestibular receptors of various vertebrates.

It is well known that the frog's vestibular nerve also contains efferent fibers whose cell bodies are located in the brain stem and the cerebellum (Hillman, 1969; Llinás and Precht, 1969). Previous physiological studies (Schmidt, 1963; Llinás and Precht, 1969) have shown that spontaneous action potentials can be recorded from fibers in the VIIIth nerve after complete deafferentation on the side of the recording. These action potentials can be activated with short latencies of approximately 3 msec after stimulation of the ipsilateral VIIIth nerve and with longer latencies after contralateral VIIIth nerve stimulation. Furthermore, the discharge of the efferent fibers recorded on the deafferented side can be increased by applying rotatory stimulation in the direction contralateral to the recording electrode. Thus, labyrinthine stimulation by itself is able to modulate the firing frequency of the efferent vestibular system. The present experiments give further information concerning some of the dynamic properties of the efferent fibers in response to horizontal angular acceleration. Since both labyrinths remained intact, most of the efferent units showed an increase in firing on rotation in either direction, indicating that both labyrinths converge onto the cells of origin of efferent fibers. Some of the efferent fibers showed a resting discharge in the absence of stimulation suggesting that the efferent system is at least partly tonic in nature. Since most of the previous studies have been done under anesthesia, the importance of tonic

resting discharge may have been underestimated due to the depressor actions of anesthesia. The same argument holds for the threshold for frequency increase in response to rotational stimulation. Although this study confirms that efferent fibers in general have higher thresholds, it was found that the thresholds of a few units were very close to those of afferent fibers. It has frequently been observed that efferent vestibular fibers respond to stimuli other than labyrinthine, such as passive movement of limbs and cutaneous stimulation (Schmidt, 1963; Llinás and Precht, 1969). Thus, the delayed and irregular decay of the discharge rate of the efferent fiber after constant velocity of rotation is reached may be explained on the basis of concomitant extralabyrinthine stimulation.

Recently another interesting observation has been made on the extralabyrinthine activation of efferent vestibular fibers. As described by Dichgans *et al.* (1970) and Schmidt *et al.* (1970), the discharge frequency of efferent vestibular fibers in goldfish and rabbit is modulated in close relationship with saccadic eye movements. The saccadic modulation of efferent discharge is independent of proprioceptive afferents from the eye muscles since it persists after paralyzing the animals and since it commences prior to the onset of the actual eye movement. The coupling of efferent vestibular activity with the central optokinetic mechanisms could be important in the regulation of the interaction between vestibularly and optokinetically induced eye movements. The fact that the efferent signal occurs about 100 msec prior to the onset of the optokinetically induced or spontaneously occurring saccades is of particular interest in this respect. At present it is not established whether the fibers that show correlation with saccades are exclusively efferent in nature or if some of them are afferent units. Klinke (1970) has claimed that the recordings he made during optokinetic stimulation originated from afferent fibers. The latter change their discharge rate several seconds after the stimulus pattern has begun to move, a finding that may be explained by the action of efferent fibers which change the sensitivity of the receptor cells. The change in discharge frequency of afferent fibers caused by optokinetic activation is such that it would compensate for the change that would have occurred due to labyrinthine stimulation had the animal been allowed to move in response to the visual stimulus. Thus, the efferent system would tend to keep the discharge frequency of a given afferent fiber fairly constant. The direction dependent changes found in afferent fibers by Klinke (1970) are in keeping with the finding that synchronous electrical activation of the efferent system causes a decrease in spontaneous firing of some afferent fibers, which indirectly suggests that the efferent system is inhibitory in nature as described by Llinás and Precht (1969). It should be emphasized, however, that even with electrical stimulation of the efferent vestibular system only a certain percentage of afferent fibers shows significant changes in frequency of firing. This may be caused by the fact that the number of efferent fibers is indeed rather small (Gazek *et al.*, 1965; Hillman, 1969).

Although a final conclusion regarding the functional meaning of the vestibular efferent system appears to be premature, it can be stated that various other sensory inputs besides the labyrinthine are able to influence the vestibular system at the receptor level via efferent fibers. Amongst them, the function of the optokinetically induced changes may soon be understood. As for the labyrinthine effects on the efferent fiber system, they probably serve as a feedback system

which, in the case of the ipsilateral loop, would be partly responsible for the frequency adaptation of some of the afferent fibers. In the case where activation of the inhibitory efferent fibers occurs during contralateral rotation, the efferent system may serve to sharpen the depressor effect produced by the directional sensitivity of the hair cells. The functional description of efferent vestibular fibers by means of physiological stimulation is, finally, very important in deciding whether a particular fiber is indeed efferent in nature. Bracchi (personal communication) has observed that following peripheral electrical stimulation of the vestibular nerve, a response similar to the dorsal root reflex (Toennies, 1938) may be recorded peripherally after a central delay. This type of phenomenon complicates the identification of efferent fibers when only the latter criterion is utilized.

APPENDIX

By M. Clarke, Division of Neurobiology, Department of Physiology & Biophysics, University of Iowa, Iowa City.

The dynamic properties of the vestibular nerve fibers of different vertebrates have been modeled in a variety of ways in the last 30 years. One of the most widely used models today regards the mechanical properties of the semicircular canal as analogous to those of a torsion pendulum, the properties of which were derived from electrical recordings of VIIIth nerve activity (Groen *et al.*, 1952). Given that the dynamic properties of the different vestibular fibers have been shown in this paper to be rather dissimilar, it is our feeling that no single process can directly explain these disparities. In fact such disparities can be so significant that the mechanical properties of a torsion pendulum model cannot be derived from their activity.

The present appendix offers a modification to the torsion pendulum model which takes into consideration some of the above discrepancies and is in keeping with the experimental findings reported in this and other papers (Steinhausen, 1931, 1933; Groen *et al.*, 1952). The model to be presented is not in agreement with the view that the vestibular fibers provide velocity information over a mid-frequency range with a lower frequency limit determined by the viscoelastic time constant of the cupula (Jones and Milsum, 1965). Instead, on the basis of experimental data, it is proposed that fibers having rather short time constants to a step input simulate acceleration channels, while fibers having long time constants simulate velocity channels. The experimental finding that the fiber responses recorded in the VIIIth nerve are dissimilar indicates, given that all receptor cells are type II, that an encoder mechanism in each nerve fiber may be the factor responsible for the difference in dynamic properties. A very clear example of such a situation is that found between tonic and phasic crayfish stretch receptors. There, the main difference between receptors is not at the transduction level but at the level of the encoder (Nakajima and Onodera, 1969a, b). Conceptually it is simpler to postulate that the receptor cells have basically similar structure and function, and that the dynamic properties of the encoder determine the nature of the information transferred by the vestibular afferents.

Figure 16 illustrates how two different responses may result from the stimulation of one hair cell having two afferent terminals with different spike adaptation mechanisms. In this diagram the cupula and endolymph response to an acceleration is represented by a torsion pendulum model. Since the viscoelastic time constant of a torsion pendulum should not vary over its length, the time constant of all hair cells would be the same regardless of their positions in the cupula. The transduction then occurs through the production of a generator potential by the deflection of stereo- and kinocilium and the subsequent release of a chemical transmitter substance. This generator potential should have a similar time course throughout the receptor cell population and should reflect the time constant of the bending of the ciliary system in these cells. Since the encoder properties of the afferent fibers include the rate-sensitive component due to spike adaptation dynamics, short time constant responses must be associated with rapidly adapting terminals, while long time constants must be associated with slowly adapting fibers. These time constants are undoubtedly short term effects associated with the rate of adaptation and with ionic mechanisms such as sodium inactivation by depolarization and the presence of electrogenic pumps (Nakajima and Onodera, 1969a, b).

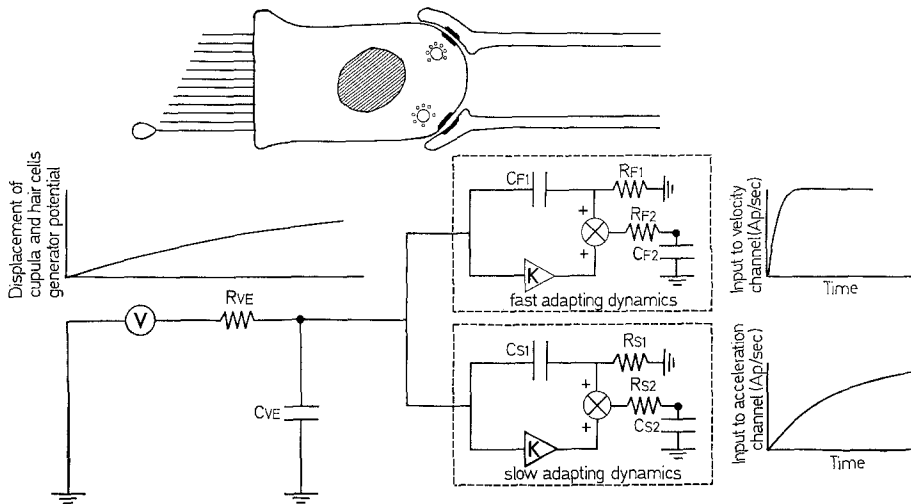


Fig. 16. Schematic diagram of a hair cell with slow and fast adapting primary nerve fibers and equivalent circuit model. Cupula deflection, hair cell deflection, and generator potential are represented by a capacitor (C_{VE}) which is in series with a resistor (R_{VE}) chosen to give a very long time constant when a step input of acceleration (V) is applied. Differentiators in series with resistor-capacitor combinations represent slow and fast adapting dynamics of the primary nerve fibers. R_{S1} , C_{S1} and R_{F1} , C_{F1} are the elements of the differentiators for slow and fast adapting fibers respectively. R_{S2} , C_{S2} and R_{F2} , C_{F2} are the elements of the integrators for slow and fast adapting fibers respectively. K represents a gain constant. The dynamic properties of fast and slow adapting fibers are represented by the outputs of capacitors (C_{F2} and C_{S2}) to give short and long time constants respectively. AP/sec, action potentials per second

Conceptually we can assume, given that a step input of acceleration results in an exponentially rising displacement of the cupula, that the time course of the neural response is to be determined by the viscoelastic properties of the cupula and endolymph. The hair cells, likewise, would generate a response with a similar time course (viscous inertial time constant is neglected in this analysis). The time constant of the response would ultimately relate to the time constant of the encoder system.

In Fig. 16a short and a long time constant response are shown. If one assumes that the viscoelastic time constant of the cupula and endolymph is very long (20—30 sec) as observed by Steinhausen the initial time course of cupula displacement approximates a ramp input for the rate sensitive portion. The displacement portion maintains the constant step response when the rate of rise becomes more exponential. The adaptation one observes in response to an acceleration step of long duration is a long lasting process and appears to show no rate sensitivity.

One such class of fibers can be characterized as having rather short time constants to a step or impulse input, properties which simulate acceleration detection channels. The second class would then be composed of fibers with long time constants which simulate velocity detection channels. Mathematically the dynamic properties of these fibers can for the most part be described with an expression containing one exponential term, with a range of time constants from 1—10 sec and modified by a non-linear component. In this respect close-to-linear units were represented by one exponential term experimentally determined by a semi-log plot of rise and fall frequency ranges to a step and impulse rotatory stimulus. The frequent encounter of close to linear fibers with short time constants implies that a saturation or 'clipping' process is not operant as an explanation for the discrepancy between the brevity of the response as compared with the time constant of the cupula. This phenomenon implies, on the other hand, that when a step input of acceleration is applied, a process analogous to the charging of an RC network occurs with a time constant that can range from less than 1 sec

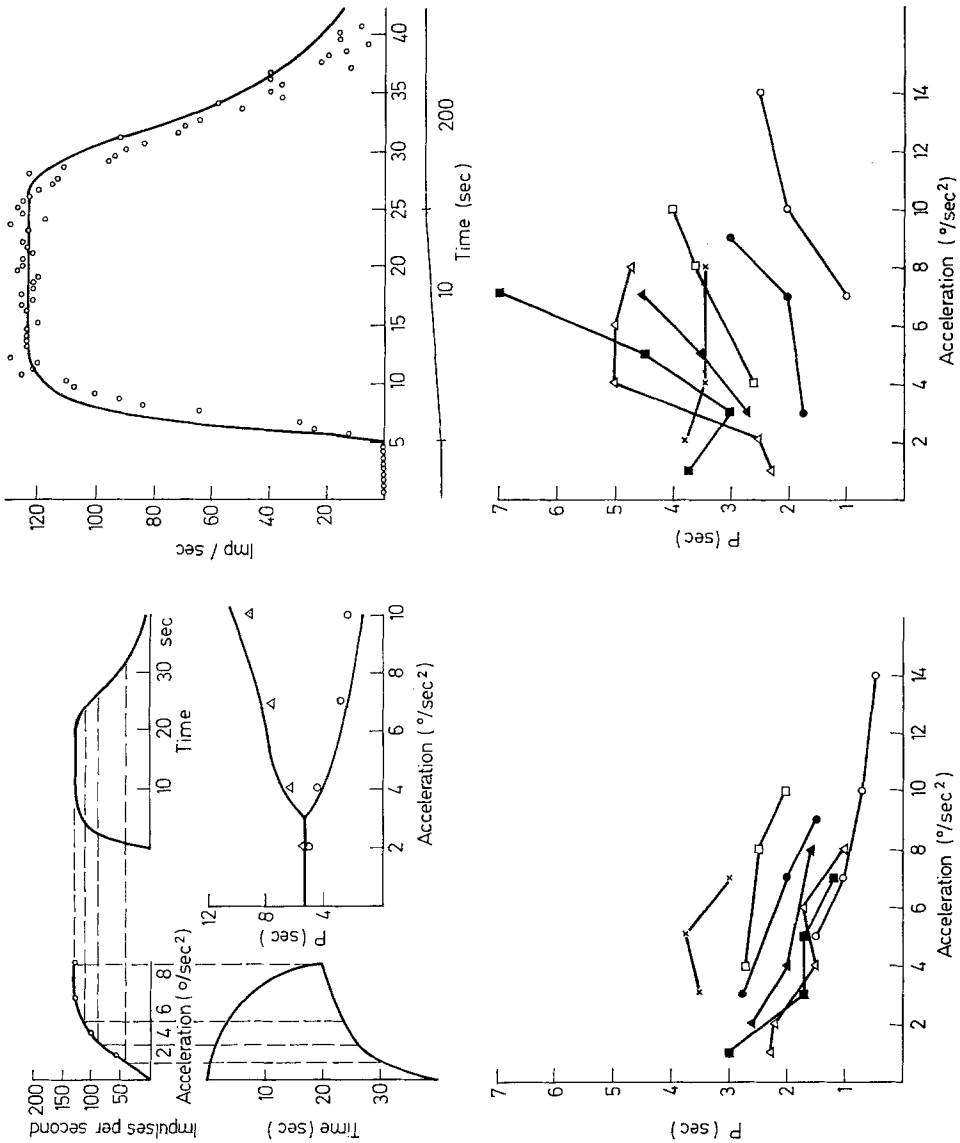


Fig. 17. Diagrams showing the derivation of theoretical responses to steps of acceleration and plots of experimental and theoretical values of p , for the rising and falling phases of the responses. Upper left section shows the modification of a theoretical input of cupula deviation by a non-linearity which was obtained from experimental data. Circles and triangles are calculated values of p for rising and falling phases respectively for individual units plotted against acceleration. The lines represent theoretical values. P is the apparent time constant. In the upper right frequency diagram, a theoretical response (line curve) and an actual response (circles) for the same unit illustrate the fast rising phase and the prolonged falling phase. In the lower diagrams are the experimental values of p for the rising and falling phases respectively, for individual units plotted against acceleration

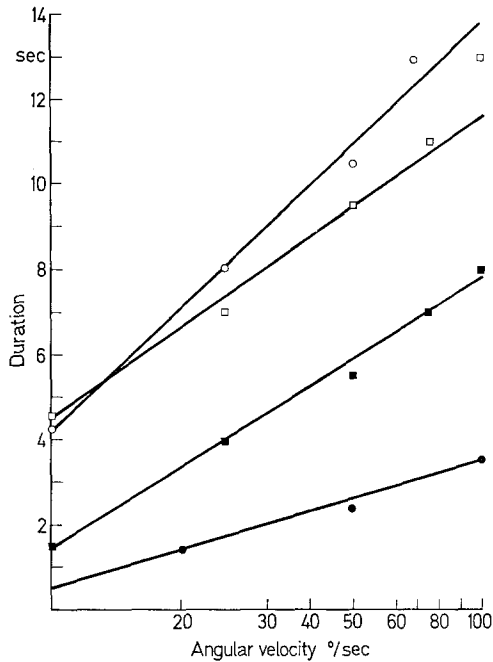


Fig. 18. *Experimental and theoretical values of duration vs angular velocity following sudden arrests of rotating turntable.* Experimental points are fitted by lines representing values calculated with time constants derived from step responses

to 10 sec. Although non-linear units operate similarly to linear units following small amplitude inputs, with larger inputs these responses are limited by the non-linearities. The final product is a shortening of the apparent time constant of the rising phase to a step of acceleration and a lengthening of the apparent time constant of the falling phase, both of which are related to the stimulus intensity (Figs. 17 and 12B).

To understand this process better, one can view the overall vestibular nerve response as an exponential input to a non-linearity as illustrated in Fig. 17. The model's non-linear input-output relation can be derived from steady state conditions by plotting the maximum output vs. the input acceleration. The time constant of the linear exponential term would be derivable from the responses obtained by using small accelerations. Figure 17 shows the analysis of an idealized experimental response including the calculated p values for the rising and falling phases of the responses to steps of acceleration for a non-linear unit. Mathematical consideration of impulse acceleration inputs sufficiently large to cause the units to operate non-linearly supports the model. A semi-logarithmic plot of velocity vs. duration for linear and non-linear units results in a linear relation. The slope of this line is the time constant, a value which is comparable to the time constants obtained for the same units in linear ranges. Figure 18 shows the durations calculated from formula 1 using the time constants derived from the step responses and the experimental values of four units. The model predicts that the durations (T) are a function of the velocity step V and the threshold E in formula 1

$$T = \tau \ln \frac{KV}{E}$$

where K is a constant and τ is the time constant. Note that the threshold non-linearity and not the static input-output non-linearity determines the duration, since the value of the output around threshold is in a more linear range of the non-linear characteristic.

A model which treats the response decline to a prolonged stimulus without altering the system's response to a short lasting stimulus is now proposed for the adapting vestibular

fibers. Two separate elements are assumed to be present in the system: (i) the adaptation dynamics consisting of a gain which is a function of the duration of the stimulus and (ii) the basic properties of the system which undergo little change when a prolonged stimulus is applied. The presence of a gain, dependent upon the duration of the stimulus and the presence of static non-linearities, precludes the use of sinusoidal analysis to obtain linear time invariant transfer functions. Furthermore, a study underway strongly supports the view that linear time invariant transfer functions obtained from sinusoidal stimulation of neurophysiological systems cannot be used to predict physiological responses in the time domain.

The fact that the time course of the rising phase of the response evoked by a step of acceleration superimposed upon an initial prolonged step shows little change from that produced by the initial step, indicates that the properties of the system undergo no apparent change during prolonged stimulation. Making the gain of the system inversely proportional to the duration of the stimulus accounts for the fact that a prolonged stimulus in one direction reduces the subsequent response to a stimulus in the same direction. This phenomenon was noted by Hallpike and Hood (1953) in their analysis of the subjective response of humans. In their discussion on adaptation, these authors note that the system's ability to respond to a second stimulus superimposed upon the first depends upon the duration of the first stimulus. The model proposed here seems thus to be an improvement over the differentiator model, which predicts that the adaptation which can be observed with prolonged stimuli is also responsible for phenomena such as the undershoot that may occur when a short lasting stimulus is applied (Young, 1969). This latter model predicts that the system's ability to respond to a second stimulus superimposed upon a prolonged conditioning stimulus will not be affected by the duration of the conditioning stimulus. Furthermore, the differentiator model predicts an undershoot when the step of acceleration is terminated. If a second step of acceleration were to be applied soon after the first was removed, partial or nearly complete cancellation would occur, depending upon the interval between stimuli. The differentiator model predicts that when the step of acceleration is terminated the rapidity with which the response undershoots, as measured by the p value method, will be greatest with prolonged stimulation. Also, if the response is terminated during the declining phase of the response to a prolonged stimulus, the p value associated with the termination of the stimulus will be less than the p value of the initial rising phase of the response. In the experimental data on the VIIIth nerve of the frog, the response was not seen to fall off abruptly. The values of p for the falling phases are usually larger than the p values of the rising phase of the step response. The durations of the impulse responses are predictable by the integrating resistor capacitor model of the basic properties of the system. In fact, Young (1969) notes that his differentiator model fails to predict the durations greater than 20 sec encountered in human subjective response for impulses of acceleration (Van Egmond *et al.*, 1949), since the impulse response of his model crosses zero at 20 sec. In the data of Van Egmond *et al.* (1949) a duration of 20 sec corresponds to a step of velocity of $10^\circ/\text{sec}$, extrapolating from the graph on page 4, Fig. 2. This model accounts for about 1/7 of the range of stimuli employed.

The model for the non-linearities of units showing adaptation predicts that the non-linearity relating the steady state input-output relation of the system can minimize adaptation effects. To better understand this process, one can view the overall response of a single nerve fiber as resulting from a linear adapting response that is modified by a non-linearity at higher stimulus intensities. The model's non-linear input-output relation can be derived from steady state conditions by plotting the maximum output vs. the input acceleration. This reduction in adaptation is more prominent when larger inputs are applied since the input-output transformation takes place over a more non-linear range. Figure 19 shows a plot of adaptation calculated as the ratio of the response at a fixed time to the peak response vs. acceleration for non-linear nerve fibers. Qualitatively the decline in adaptation with increasing stimuli fits the model. The adaptation in linear units is independent of the stimulus intensity as predicted by the model. Figure 7 in this paper illustrates an example of a linear unit showing adaptation.

Several investigators have tried unsuccessfully to derive cupula characteristics either from gross recordings of VIIIth nerve activity or from central events related to semicircular canal activity. The mathematical analysis performed on the gross response of the frog vestibular nerve yields results that conflict with the analysis done on single nerve fibers (Ledoux, 1958). A value of 6 sec was obtained from semilogarithmic plots of step and impulse data for the

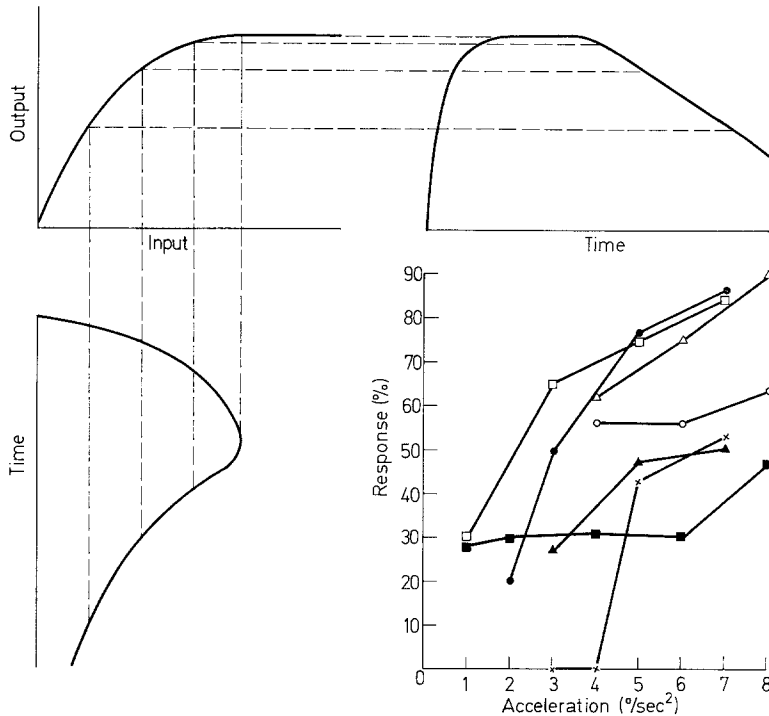


Fig. 19. *Non-linear effects on adaptation vs acceleration.* A rapidly adapting unit at low stimulus intensities is transformed by the non-linear input-output characteristic to a slowly adapting unit at higher stimulus intensities. Graph at lower right corner illustrates the reduction in adaptation as a function of stimulus intensity for individual units. The ordinate represents the ratio of the response at 15 sec to the peak response. Abscissa represents acceleration. A horizontal line at 100% would correspond to no adaptation

dominant time constant. This was assumed to be mathematically analogous to the viscoelastic time constant in the torsion pendulum model, but it conflicts with the fact that most time constants obtained from single fibers are between 2 and 3 sec. Similar problems were encountered by investigators who attempted to derive a viscoelastic time constant for the cupula from recordings taken during nystagmus and during subjective human response (Jones and Milsum, 1965; Young, 1969). A single value of 16 sec was obtained from mathematical considerations (Young, 1969). This estimate is more than twice the average value of the time constant reported here from single units in the frog and reported by Goldberg and Fernandez (1969) in the monkey.

Acknowledgement: The present research was supported by a special grant from the Institute for Biomedical Research, AMA/ERF.

References

- Burlet, H.M. de: Zur vergleichenden Anatomie der Labyrinthinnervation. *J. comp. Neurol.* **47**, 155—169 (1929).
- Clark, B.: Thresholds for the perception of angular acceleration in man. *Aerospace Med.* **38**, 443—450 (1967).
- Dichgans, J., Wist, E.R., Schmidt, C.L.: Modulation neuronaler Spontanaktivität im N. vestibularis durch optomotorische Impulse beim Kaninchen. *Pflügers Arch.* **319**, R154 (1970).
- Ewald, J.R.: Physiologische Untersuchungen über das Endorgan des N. Oktavus. Wiesbaden: Bergmann 1892.

- Gazek, R. R., Nomura, Y., Balogh, K.: Acetylcholinesterase activity in the efferent fibers of the stato-acoustic nerve. *Acta oto-laryng. (Stockh.)* **59**, 541 (1965).
- Gernandt, B. E.: Response of mammalian vestibular neurons to horizontal rotation and caloric stimulation. *J. Neurophysiol.* **12**, 173—184 (1949).
- Gleisner, L., Henriksson, N. G.: Efferent and afferent activity pattern in the vestibular nerve of the frog. *Acta oto-laryng. (Stockh.) (Suppl. 192)* **58**, 90—103 (1963).
- Goldberg, J. M., Fernandez, C.: Responses of first-order vestibular afferents of the squirrel monkey to angular acceleration. *Conf. on Systems Analysis Approach to Neurophysiological Problems*. Brainerd, Minn. 1969.
- Groen, J. J., Lowenstein, O., Vendrik, A. J. H.: The mechanical analysis of the responses from the endorgans of the horizontal semicircular canal in the isolated elasmobranch labyrinth. *J. Physiol. (Lond.)* **117**, 329—346 (1952).
- Hallpike, C. S., Hood, J. D.: Fatigue and adaptation of the cupular mechanism of the human horizontal semicircular canal: An experimental investigation. *Proc. roy. Soc. B.* **141**, 542—561 (1953).
- Hillman, D. E.: Light and electron microscopical study of the relationships between the cerebellum and the vestibular organ of the frog. *Exp. Brain Res.* **9**, 1—15 (1969).
- Jones, G. M., Milsum, J. H.: Spatial and dynamic aspects of visual fixation. *IEEE Trans. Bio-med. Eng.* **12**, 54—62 (1965).
- Jung, R., Kornhuber, H. H.: Results of electro-nystagmography in man. The value of optokinetic, vestibular and spontaneous nystagmus for neurologic diagnosis and research. In: *The Oculomotor System*, pp. 428—477. Ed. by M. B. Bender. New York: Harper and Row 1964.
- Klinke, R.: Efferent influence on the vestibular organ during active movements of the body. *Pflügers Arch.* **318**, 325—332 (1970).
- Ledoux, A.: Activité électrique des nerfs des canaux semicirculaires du saccule et de l'utricule chez la grenouille. *Acta oto-rhino-laryng. belg.* **3**, 335—349 (1949).
- Les canaux semicirculaires. Etude électrophysiologique. Contribution à l'uniformisation des épreuves vestibulaires. Essai d'interprétation de la semiologie vestibulaire. *Acta oto-rhino-laryng. belg.* **12**, 109—348 (1958).
- L'adaptation du système vestibulaire périphérique. *Acta oto-laryng. (Stockh.)* **53**, 307—316 (1961).
- Llinás, R., Precht, W.: The inhibitory vestibular efferent system and its relation to the cerebellum in the frog. *Exp. Brain Res.* **9**, 16—29 (1969).
- — Clarke, M.: Cerebellar Purkinje cell responses to physiological stimulation of the vestibular system in the frog. *Exp. Brain Res.* **13**, 408—431 (1971).
- Lowenstein, O.: The effect of galvanic polarization on the impulse discharge from sense endings in the isolated labyrinth of the thornback ray (*Raja clavata*). *J. Physiol. (Lond.)* **127**, 104—117 (1955).
- Peripheral mechanisms of equilibrium. *Brit. med. Bull.* **12**, 114—118 (1956).
- Sand, A.: The mechanism of the semicircular canal. A study of the responses of single-fibre preparations to angular accelerations and rotation at constant speed. *Proc. roy. Soc. B.* **129**, 256—275 (1940a).
- — The individual and integrated activity of the semicircular canals of the elasmobranch labyrinth. *J. Physiol. (Lond.)* **99**, 89—101 (1940b).
- Nakajima, S., Onodera, K.: Membrane properties of the stretch receptor neurons of crayfish with particular reference to the mechanisms of sensory adaptation. *J. Physiol. (Lond.)* **200**, 161—185 (1969a).
- — Adaptation of the generator potential in the crayfish stretch receptors under constant length and constant tension. *J. Physiol. (Lond.)* **200**, 187—204 (1969b).
- Precht, W., Grippo, J., Richter, A.: Effect of horizontal angular acceleration on neurons in the abducens nucleus. *Brain Res.* **5**, 527—531 (1967).
- Richter, A., Grippo, J.: Responses of neurones in cat's abducens nuclei to horizontal angular acceleration. *Pflügers Arch.* **309**, 285—309 (1969).
- Schmidt, C. L., Wist, E. R., Dichgans, J.: Alternierender Spontan-nystagmus, optokinetischer und vestibulärer Nystagmus und ihre Beziehungen zu rhythmischen Modulationen der Spontanaktivität im N. vestibularis beim Goldfisch. *Pflügers Arch.* **319**, R155 (1970).

- Schmidt, R.F.: Frog labyrinthine efferent impulses. *Acta oto-laryng.* (Stockh.) **56**, 51—64 (1963).
- Schoen, L.: Mikroableitungen einzelner zentraler Vestibularisneurone von Knochenfischen bei Statolithenreizen. *Z. vergl. Physiol.* **39**, 399—417 (1957).
- Shimazu, H., Precht, W.: Tonic and kinetic responses of cat's vestibular neurons to horizontal angular acceleration. *J. Neurophysiol.* **28**, 991—1013 (1965).
- Steinhausen, W.: Über den Nachweis der Bewegung der Cupula in der intakten Bogengangsampulle des Labyrinthes bei der natürlichen rotatorischen und calorischen Reizung. *Pflügers Arch. ges. Physiol.* **228**, 322—328 (1931).
- Über die Beobachtung der Cupula in den Bogengangsampullen des lebenden Hechts. *Pflügers Arch. ges. Physiol.* **232**, 500—512 (1933).
- Szentágothai, J.: The elementary vestibulo-ocular reflex arc. *J. Neurophysiol.* **13**, 395—407 (1950).
- Toennies, J.F.: Reflex discharges from the spinal cord over dorsal roots. *J. Neurophysiol.* **1**, 378—390 (1938).
- Trincker, D.: Physiologie des Gleichgewichtsorgans. In: *Hals-Nasen-Ohren-Heilkunde*, Bd. III, T. 1. Ed. by J. Berendes, R. Link, F. Zöllner. Stuttgart: Georg Thieme 1965.
- Van Egmond, A.A.J., Groen, J.J., Jongkees, L.B.W.: The mechanics of the semicircular canal. *J. Physiol. (Lond.)* **110**, 1—17 (1949).
- Young, L.R.: Biocybernetics, of the vestibular system. In: *Biocybernetics of the Central Nervous System*, pp. 79—117. Ed. by L.D. Proctor. Boston: Little, Brown & Co. 1969.

Dr. W. Precht
Max-Planck-Institut
für Hirnforschung
Neurobiolog. Abt.
6 — Frankfurt/M. (West Germany)
Deutschordenstraße 46

Dr. R. Llinás
Mr. M. Clarke
Division of Neurobiology
Dept. of Physiology & Biophysics
University of Iowa
Iowa City, Iowa 52240 (USA)